Extended Abstracts of the 2007 International Conference on Solid State Devices and Materials, Tsukuba, 2007, pp. 1116-1117

I-8-5

Improved Photoconduction Effects of Nanometer-Sized Si Dot Multilayers

Yoshiyuki Hirano[1], Susumu Yamazaki[2] and Nobuyoshi Koshida[2]

[1]NHK Science and Technical Research Laboratories
1-10-11, Kinuta, Setagaya-ku, Tokyo 157-8510, Japan
Phone: +81-3-5494-3212 Fax: +81-3-5494-3278 E-mail: hirano.y-eg@nhk.or.jp
[2]Tokyo University of Agriculture and Technology
2-24-16, Naka-machi, Koganei, Tokyo 184-8588, Japan

1. Introduction

With the aim of possible application to ultrahigh sensitive solid-state imaging sensor and highly functional image sensor, we have been conducting fundamental research on photoconductive films consisting of nanometer-sized silicon dots (Si nanodots).

Si nanodots are expected as a novel photoconductive material from the following reasons: (1) Spectral response characteristics are controlled by changing the bandgap with the crystal size of the Si nanodot. (2) Impact ionization rate of the single crystal Si nanodot is thought to be higher than that of amorphous Se and amorphous Si. (3) The impact ionization rate should be further enhanced by using the semi-ballistic carrier transport[1] induced in the Si nanodot/SiO_2 system.

We have reported that multilayered Si nanodots (Si-nanodot multilayer) with the dot size of 3-5 nm, which are prepared by repeating low-pressure chemical vapor deposition for dot formation and subsequent thermal oxidation for dot isolation, exhibits a significant photosensitivity in the photon energy region above 2 eV.[2] The quantum efficiency of the Si-nanodot multilayer was, however, much lower than that of conventional photoconductive materials.

In this study, the relationship between the fabrication condition and photoconductive properties has been investigated for Si-nanodot multilayers. Key issues for the improvement in the quantum efficiency are clarified.

2. Experimental

Si-nanodot multilayers were prepared through the following procedure. (1) After RCA cleaning of n-type c-Si (100) wafers with a resistivity of 0.01 Ωcm, the wafers were oxidized in O_2 at 600 or 800 ^oC to grow a <1-nm-thick SiO_2 layer. The oxidation pressure and time were fixed at 8 Torr and 120 sec, respectively. (2) A single layer of Si nanodots was deposited using LPCVD from SiH_4 on the oxidized Si substrates immediately after the oxidation process. The deposition pressure, temperature and time were fixed at 6 Torr, 545 ^oC and 30 sec, respectively. (3) Prepared Si nanodots were oxidized under the same condition as the process (1) to cover each dot surface with a tunnel SiO_2 film (<1-nm-thick). (4) Such deposition/oxidation steps were repeated for 60 times. (5) Finally, the samples were annealed in N_2 at 1000 ^oC for 60 min to reduce defects in Si/SiO_2 interface region.

The dot size and density of Si-nanodot multilayers were determined from the transmission-electron-microscopy (TEM).

The photoconductive characteristics of the Si-nanodot multilayers were measured using a cell structure with semi-transparent Au electrodes deposited on the Si-nanodot multilayer. Monochromic light with a power of 50 $\mu W/cm^2$ was irradiated from the Au electrode side with the Si substrate positively biased.

3. Results and Discussion

Cross-sectional TEM images for Si-nanodot multilayers formed with the oxidation temperature of 800 ^oC (sample A) and 600 ^oC (sample B) are shown in **Fig. 1**. A Si nanodot observed in both samples is a spherical single crystal and separated by SiO_2 from each other. The dot size distributions estimated from the TEM images are shown in **Fig. 2**. The density of Si nanodots for sample B is about two times as high as that for the sample A.

Figure 3 shows current-voltage characteristics for sample A and B under the illumination by 4.1 eV monochromic light and in the dark. The photocurrent for sample B is about an order of magnitude as large as that for sample A, indicating the tunneling probability of photo-excited carriers between nanodots is increased, since the distance between Si nanodots for sample B is shorter than that for sample A. The quantum efficiency at an applied voltage of 3V for sample B is about 34% which is almost comparable to conventional photoconductive materials. The quantum efficiency, however, tends to decrease at lower applied voltages possibly due to carrier trapping by dangling bonds at the Si nanodot interfaces.

To terminate the residual Si dangling bonds, sample B was annealed at 300 ^oC for 120 min in the ambience of atomic hydrogen species generated through cracking hydrogen molecules by a tungsten hot filament (temperature: 1500 ^oC) at a pressure of 5 Torr. In **Fig. 4** are shown the ESR spectra before and after the atomic hydrogen annealing. The ESR signal at g=2.0055, which is attributed to Si dangling bonds, for the sample after annealing (sample C) is much smaller than that for sample B.

Figure 5 shows the current-voltage characteristics for sample B and C. Though the dark current for both samples is comparable with each other, the photocurrent for sample C is about two orders of magnitude higher than that for sample B and quantum efficiency of 51% is achieved at an applied voltage of 1V. This improvement in the quantum efficiency can be explained as a result of hydrogen termination of the dangling bonds followed by sufficient suppression of recombination loss of photo-excited carriers.

4. Conclusions

The photoconduction quantum efficiency of the Si nanodot film was extremely improved by increasing spatial density of Si nanodots and passivating interfacial dangling bonds with hydrogen termination. Under appropriate processing parameters, high quantum efficiency over 50% was obtained even at low bias voltages. Further enhanced photoconductivity would be attained by the assistance of the electric field effect.

References

[1] N. Koshida, X. Sheng, and T. Komoda, Appl. Surf. Sci. **146** (1999) 371.

[2] Y. Hirano, F. Sato, S. Aihara, N. Saito, S. Miyazaki, and M. Hirose, Appl. Phys. Lett., **79** (2001) 2255.

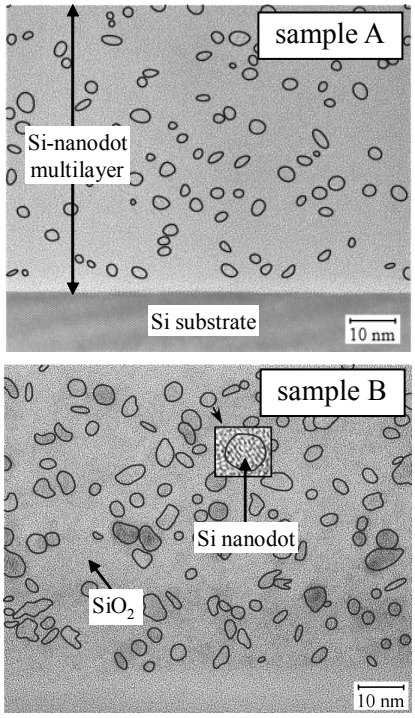

Fig. 1. Cross-sectional TEM images for Si-nanodot multilayers with oxidation temperature of 800 °C (sample A) and 600 °C (sample B).

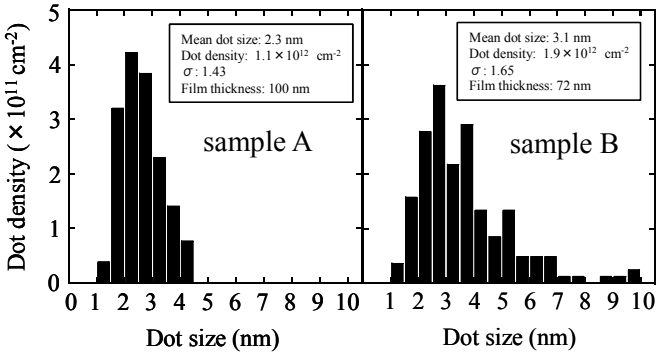

Fig. 2. Dot size distributions estimated from TEM images.

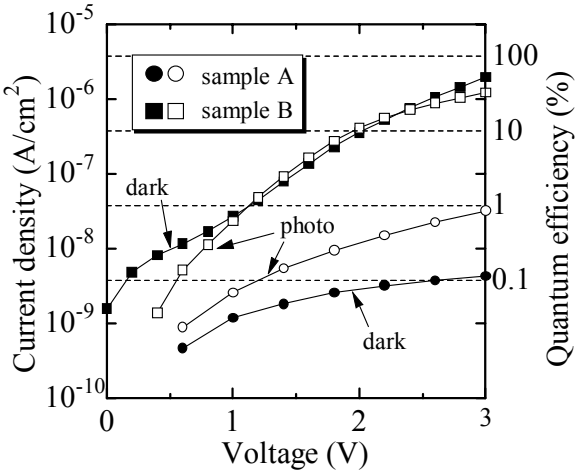

Fig. 3. Current-voltage characteristics for sample A and B under illumination by 4.1 eV monochromic light.

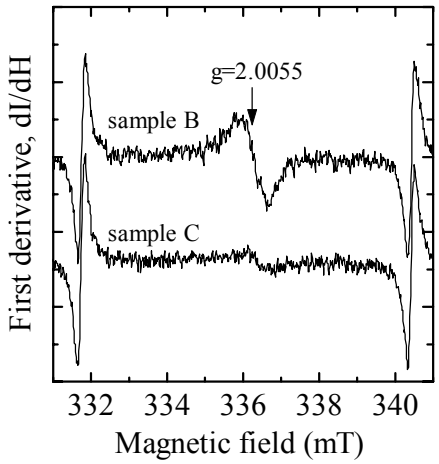

Fig. 4. ESR spectra before atomic hydrogen annealing (sample B) and after atomic hydrogen annealing (sample C).

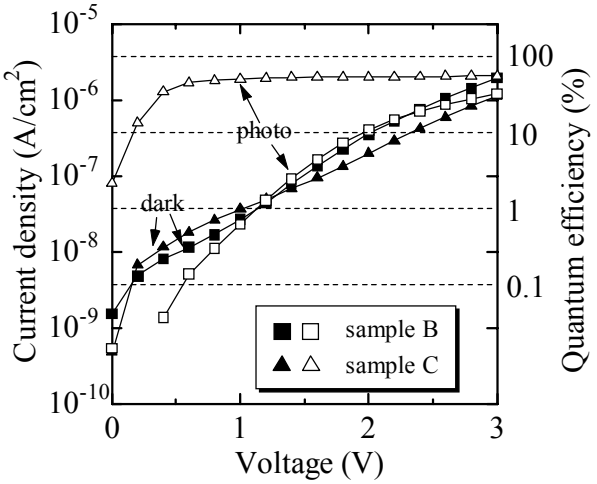

Fig. 5. Current-voltage characteristics for sample B and C under illumination by 4.1 eV monochromic light.